MEASUREMENT OF PILOT DESCRIBING FUNCTIONS FROM FLIGHT TEST DATA
WITH AN EXAMPLE FROM GEMINI X

By Rodney C. Wingrove* and Frederick G. Edwards*

Ames Research Center, NASA
Moffett Field, California 94035

*Research Scientist.

ABSTRACT

Under normal flight test conditions, it has been known that there is an error in measuring the pilot describing function due to a correlation of the input error signal with the pilot's output noise. It is shown in this paper that this measurement error can be reduced by shifting the input signal during the computer processing. The input signal is shifted by an amount equivalent to the pilot's time delay. This technique is based on a theoretical development which considers the fact that the measurement is constrained to only identify physically realizable systems. The simulation and identification of an example pilot model is included in this study to illustrate this technique. Also, representative data from the retrofire phase of the Gemini X flight have been analyzed and are presented to demonstrate the feasibility of using this technique with normal spacecraft operating records.

INTRODUCTION

Pilot describing functions have usually been identified from records obtained in ground-based simulators and flight tests wherein carefully controlled external forcing functions (i.e., sine waves) are used to excite the pilot vehicle system. In these analyses, the pilot's output and input are compared with the known forcing function in order to reduce errors in identification due to any correlation of the input error signal with the pilot's output noise. Reference 1 contains a good review of this previous work and summarizes the pilot describing functions measured for a variety of vehicle and control system dynamics.

Some methods proposed for pilot describing functions identification use flight test data wherein only random external disturbances (i.e., aerodynamic turbulence, propulsive disturbance, etc.) excite the pilot vehicle system. These are the so-called open-loop methods which compute the pilots describing function directly from the pilots input and output signals. In reference 2, these methods have been reviewed and the expected errors in identification have been analyzed. It was shown that there is a measurement error when using these open-loop methods due to the fact that the pilot's output noise is transferred through the control loop, appearing as a component of his input error signal, and thus is correlated with his input. It was further shown that if the pilots noise was large, as compared with the external disturbance, then the measurement error would probably be unacceptable.

During normal flight test operations there are usually no carefully controlled forcing functions and even the random external disturbance may be quite small. The purpose of this report is to present the development of a technique to reduce the error in measuring the pilot describing functions for these normal flight test operations. A brief theoretical development of this technique is included in the appendix. This technique involves shifting the time history of the input error signal during the computer processing. The input signal is shifted an amount equivalent to the pilot's time delay. As shown in the appendix, this technique could conceivably be used with any open-loop method which is constrained to only identify physically realizable systems. For the purposes of this report, this technique will be applied with two representative identification methods; cross-correlation (refs. 2 and 3) and orthogonal filters (refs. 2 and 4). Although previous studies (e.g., refs. 4 and 5) have considered the use of a time delay in the measurement of pilot describing functions, it was apparently not observed that this time delay would strongly influence the errors in identification.

In this paper, this technique of reducing measurement errors will be illustrated through the simulation and identification of a known system. This technique will also be applied to data recorded during the Gemini X flight. These results will serve to demonstrate the application of this technique for measuring the pilot describing functions using actual flight test records.

NOMENCLATURE

$c(t)$	controller deflection (output of pilot)
$e(t)$	error signal (input to pilot)
$i(t)$	external disturbance
$n(t)$	pilot noise
$R_{nn}(\tau)$	autocorrelation function of $n(t)$
t	time, sec
$Y_c(j\omega)$	controlled element
$Y_p(j\omega)$	pilot transfer function
$\hat{Y}_p(j\omega)$	measured pilot transfer function
α	exponential decay factor, sec^{-1}
λ	pure time delay used during analysis, sec
τ_c	pure time delay in Y_c, sec
τ_p	pure time delay in Y_p, sec
$\Phi_{ee}(\omega)$	power spectrum of $e(t)$
$\Phi_{nn}(\omega)$	power spectrum of $n(t)$
$\Phi_{ec}(j\omega)$	cross-power spectrum of $e(t)$ and $c(t)$

$\Phi_{en}(j\omega)$ cross-power spectrum of $e(t)$ and $n(t)$

ω frequency, rad/sec

MEASUREMENT ERROR WITH OPEN-LOOP IDENTIFICATION METHODS

Measuring pilot describing functions with open-loop identification methods is illustrated in the upper portion of figure 1. In order to

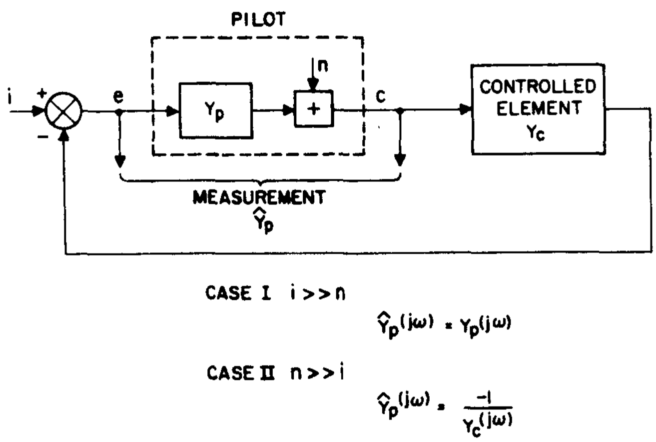

Figure 1.- Measurement of describing functions with open-loop identification methods.

determine the unknown describing function, $Y_p(j\omega)$, there must be some signal within the control loop. This signal could be the result of the disturbance source, $i(t)$, or the noise introduced by the pilot $n(t)$. Although $i(t)$ is shown in figure 1 as a time-varying command, it can also be considered (through block diagram reduction) to contain any other type of disturbance such as aerodynamics, propulsion, etc., which is external to the pilot. The pilot is assumed to be in a compensatory tracking task trying to control his output $c(t)$ in such a manner as to keep the error signal $e(t)$ near zero.

In measuring the pilot's describing function using these types of open-loop methods, previous studies (e.g., refs. 2 and 6) have shown that there is a difference between the measured describing function $\hat{Y}_p(j\omega)$ and the actual describing function $Y_p(j\omega)$ due to a correlation of $e(t)$ with $n(t)$. This can be shown using cross-spectral relationships for the estimated describing function.

$$\hat{Y}_p(j\omega) = \frac{\Phi_{ec}(j\omega)}{\Phi_{ee}(\omega)} \tag{1}$$

where $\Phi_{ec}(j\omega)$ is the cross-power spectrum between $e(t)$ and $c(t)$ and $\Phi_{ee}(\omega)$ is the power density spectrum of $e(t)$. If basic relationships are used for the closed loop system in figure 1, the cross-product can be written as the sum $\Phi_{ec}(j\omega) = Y_p(j\omega)\Phi_{ee}(j\omega) + \Phi_{en}(j\omega)$. Substituting this into equation (1), we then obtain

$$\hat{Y}_p(j\omega) = Y_p(j\omega) + \underbrace{\frac{\Phi_{en}(j\omega)}{\Phi_{ee}(\omega)}}_{\text{error}} \tag{2}$$

It can be seen that any correlation, $\Phi_{en}(j\omega)$, between $e(t)$ and $n(t)$ can contribute an error when open-loop identification methods are used. The amount of this error derived in the previous studies is illustrated on the lower portion of figure 1. For case I where $i(t)$ is much larger than $n(t)$ it has been shown that the measured describing function $\hat{Y}_p(j\omega)$ will be near the true value $Y_p(j\omega)$. However, for case II in which $n(t)$ is much larger than $i(t)$, it has been shown that the measured describing function will be very much in error, and, in fact, the identification methods will measure[1] $\hat{Y}_p(j\omega) \approx -1/Y_c(j\omega)$.

THE USE OF A TIME DELAY, λ, TO REDUCE MEASUREMENT ERRORS

Because for normal flight test conditions $n(t)$ may be large compared to $i(t)$, it is necessary to find some means of reducing the large error indicated in case II above. The theoretical development of such a technique is described in the appendix. This development considers the fact that in using time-domain identification methods, the measurement is constrained to be physically realizable. It also considers the fact that the pilot describing function is characterized by a time delay, τ_p. It is shown in the appendix that delaying the input data (see upper portion of fig. 2) by an amount λ, where $\lambda \leq \tau_p$, will reduce the measurement error.

The results from the appendix are summarized in the lower portion of figure 2. These results assume $n(t) \gg i(t)$ to illustrate the maximum errors to be expected. The rest of this section will discuss these results in detail.

Theoretical Results

As shown in the appendix, the measurement error depends upon the autocorrelation function, $R_{nn}(\tau)$, of the pilot's noise and its relation to the pilot's impulse response function (see sketch). As noted for case III in figure 2, if the spectrum of the pilot noise is near white noise, that is if $R_{nn}(\tau) = 0$ for all values of τ greater than λ, then

[1]As shown in the appendix, this is modified if Y_c is a non-minimum phase and the measurement has the constraint only to identify physically realizable systems.

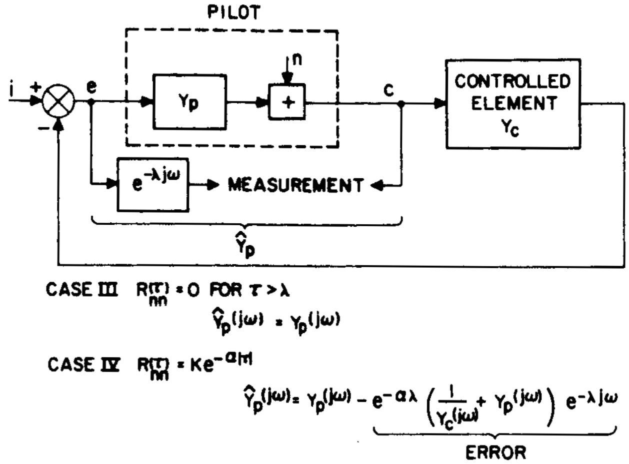

Figure 2.- Measured describing functions using a time delay; $0 \le \lambda \le \tau_p$, Y_c minimum phase, $n(t) \gg i(t)$.

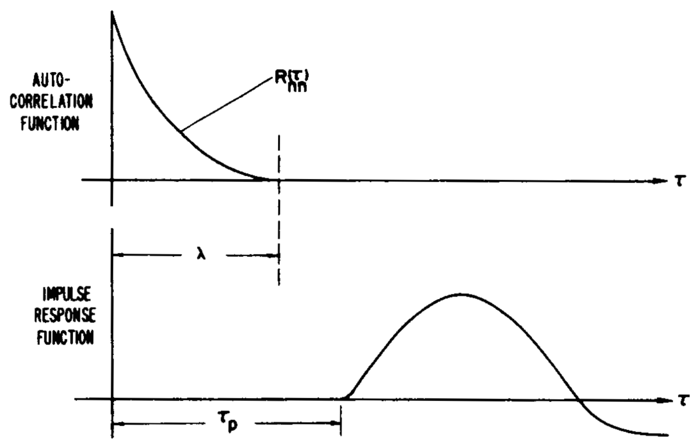

the measurement error will be zero. This result appears to be significant and has many far-reaching ramifications. The most important point is that a system describing function, $Y_p(j\omega)$, can theoretically be measured with the system excited only by the internal noise, $n(t)$.

The measured describing function will be identical to the true describing function, but only if the special conditions noted in case III are met. A more general condition is noted under case IV. Here, $R_{nn}(\tau)$, the pilot's injected noise described in terms of an autocorrelation function is assumed to take the form $R_{nn}(\tau) = Ke^{-\alpha|\tau|}$ which would be narrow-band noise. This form agrees quite well with some experimental measurements of the pilot's remnant. For instance, this exponential form with $\alpha = 5\ \text{sec}^{-1}$ agrees with the measured $n(t)$ in reference 7. The measurement error has been derived and is shown in figure 2. These latter two cases will now be illustrated by an experimental example.

Simulation Results

To illustrate the theory presented in cases III and IV, the representative control loop shown in the upper left of figure 3 was simulated,

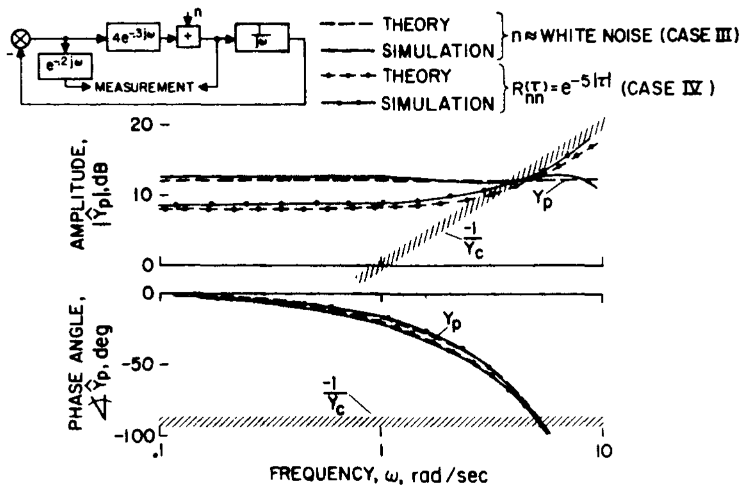

Figure 3.- Example using only internal disturbance; measurement with cross-correlation method, 15 sec run length.

and identification measurements were made on the known system. For this example, a representative pilot model and controlled element were as follows: $Y_p(j\omega) = 4e^{-0.3j\omega}$, $Y_c(j\omega) = (1/j\omega)$. These measurements were made with no external disturbance, $i(t) = 0$, and the only excitation to the system dynamics was the internal noise source, $n(t)$. A time delay of $\lambda = 0.2$ sec was used. Two forms of the noise spectrum were considered: an $n(t)$ with a spectrum which approximates white noise to illustrate case III and $R_{nn}(\tau) = e^{-5|\tau|}$ to illustrate case IV.

For case III where $n(t)$ is near white noise, the theory predicts that the measurement will identify the known system, that is $\hat{Y}_p(j\omega) = 4e^{-0.3j\omega}$. Figure 3 presents the experimental results. The measured amplitude of $\hat{Y}_p(j\omega)$ is only ±1 dB about the true value for frequencies to about 9 rad/sec and the phase angle is only ±5° about the true value. These differences are believed to be within the experimental accuracies of the simulation. These results for case III then seem to substantiate the theoretical conclusion that it is possible to measure the describing function of a system which is excited by noise $n(t)$ introduced internally within the system.

For case IV, where $R_{nn}(\tau) = e^{-5|\tau|}$, theory predicts an error in the measurement; that is,

$$\hat{Y}_p(j\omega) = \underbrace{4e^{-0.3j\omega}}_{Y_p(j\omega)} - \underbrace{0.37(j\omega + 4e^{-0.3j\omega})e^{-0.2j\omega}}_{\text{error}} \tag{3}$$

The simulation data in figure 3 for this case are again near the value predicted above by the theory. We can see from this figure the measured value of the amplitude of the describing function $\hat{Y}_p(j\omega)$ differs from the true value $Y_p(j\omega)$ in such a manner as to produce too low a value (about 4 dB below the true value) at the lower frequencies and tends to give the appearance of lead (slope = 20 dB/decade) at the higher frequencies. Actually, the measurement is tending toward $-1/Y_c(j\omega)$ as predicted by the theory. The phase angle, however, agrees quite well with the true value.

If a time delay were not used in this example, that is, if $\lambda = 0$, then the measured describing function would be $\hat{Y}_p(j\omega) = -1/Y_c(j\omega)$, as shown by the cross-hatched line in figure 3. We can note that with $\lambda = 0$ the value of the constant factor in the error term for case IV is $e^{-\alpha\lambda} = 1$. The value of this constant factor with $\lambda = 0.2$, as shown in equation (3), is $e^{-\alpha\lambda} = 0.37$. In comparing these values, we see that using $\lambda = 0.2$ resulted in approximately a 63% reduction in the magnitude of the error term (only the phase is affected by the factor $e^{-\lambda j\omega}$). Also if λ were nearer to the true value of τ_p in this example, that is, if $\lambda = 0.3$ sec, then this would have resulted in $e^{-\lambda\alpha} = 0.22$, corresponding to a 78% reduction in the magnitude of the error term.

Application

As we have just shown, using the time delay λ will reduce the measurement error due to the correlation of $n(t)$ with $e(t)$. Case IV above indicates that λ should be as large as possible in order to minimize this error. However, λ should not be much greater than τ_p because then the total measurement error will tend to increase. It appears from our experience that λ should be near the value of the pilot's effective time delay, τ_p. The pilot's effective time delay may be approximately known in some situations (i.e., ref. 1) but, in general, its value will be unknown and will depend upon the particular piloting task. One method of estimating the pilot's effective time delay (thus selecting λ) will be illustrated later in the report.

In these previous examples, the measurement errors were near the maximum to be expected since the system was excited only by the internal noise source. The addition of external disturbances (ref. 2) will tend to reduce the error in measurement. It is desirable, therefore, in applications to analyze those portions of the flight test record which have some external disturbances in order to insure the best possible measurement of Y_p.

FLIGHT TEST RESULTS FROM GEMINI X

Records taken during the Gemini flights are currently being analyzed at Ames Research Center in order to measure the pilot describing function during manned spacecraft operations. The following results, from Gemini X, will include only one example of the flight data which serves to illustrate the subject identification technique. As noted previously, in selecting the flight test data to be analyzed it is important to select a section of the record that contains the maximum number of external disturbances. This was found to be the case during the retrofire maneuver where external disturbances were introduced due to the unsymmetric ripple firing of the 4 retro-rockets.

During retrofire the pilot is controlling the attitude about each of the three axes. There is no control coupling between these axes and the pilot appears to treat them as three separate tasks. Of the three axes, the control about the yaw axis, shown in figure 4, was found to

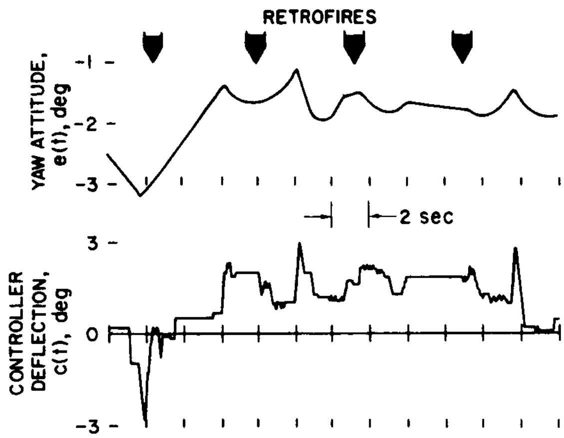

Figure 4.- Time history of yaw control task during retrofire.

contain the best consistent correlation between attitude deviations, e(t) and control stick deflections, c(t). These data for only the yaw axis control will be used to illustrate the measurement of the pilot's describing function during retrofire.

The Bode plots of the pilot describing function obtained by the cross-correlation method for the data of figure 4 are presented in figure 5. Curves of the magnitude, $|\hat{Y}_p(j\omega)|$, and phase angle, $\measuredangle \hat{Y}_p(j\omega)$, are presented as a function of frequency for two values of λ: $\lambda = 0$ and $\lambda = 0.7$ sec. Also shown by the cross-hatched line is the Bode plot for the negative inverse of the vehicle dynamics, $-1/Y_c(j\omega)$ (this line represents only an approximation because Y_c is not linear). The significance of this line was noted previously. The theory, as shown in the appendix, predicts that for $\lambda = 0$ the measured describing function $\hat{Y}_p(j\omega)$ will tend toward $-1/Y_c(j\omega)$. It should not measure this exactly, however, because of the external disturbances caused by the retro-rockets. These plots illustrate that for $\lambda = 0$, the $\hat{Y}_p(j\omega)$ does tend toward $-1/Y_c(j\omega)$ as compared with that for the measurement made with some positive value of λ; in this case $\lambda = 0.7$ sec.

Now in using this technique of measurement an important question is, "what value for λ should be used?". As noted previously λ should be near τ_p. For these data the following procedure appears promising.

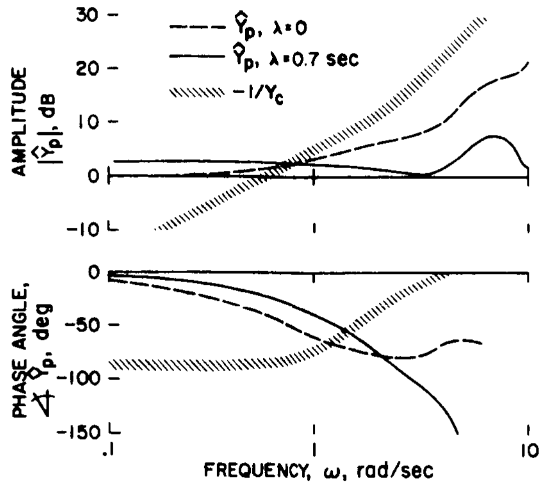

Figure 5.- Effect of time delay using cross-correlation method; yaw control during retrofire.

(1) Compute the Bode plot for a given value of λ

(2) Select the transfer function that best fits the Bode plot (i.e., $Y_p(j\omega) = Ke^{-\tau_p j\omega}$, etc.)

(3) Note the value of τ_p from (2)

These steps are repeated for several values of λ in order to determine a value of λ that corresponds to τ_p. This procedure is illustrated in figure 6 for the yaw axis task. The estimated τ_p from fairing

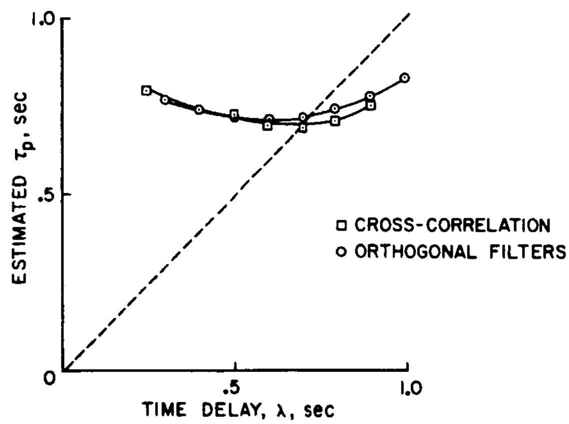

Figure 6.- Comparison of estimated time delay with λ; yaw control during retrofire.

through the Bode plots are presented as a function of λ. Data are presented for both the orthogonal filters method and the cross-correlation method. It is seen that the estimated λ is equal to the time delay,

τ_p, at $\lambda \approx 0.7$. Therefore, $\lambda = 0.7$ was selected for use in this identification analysis.

Figure 7 presents the Bode plots obtained by the cross-correlation and orthogonal filter methods. The two measurements are given for

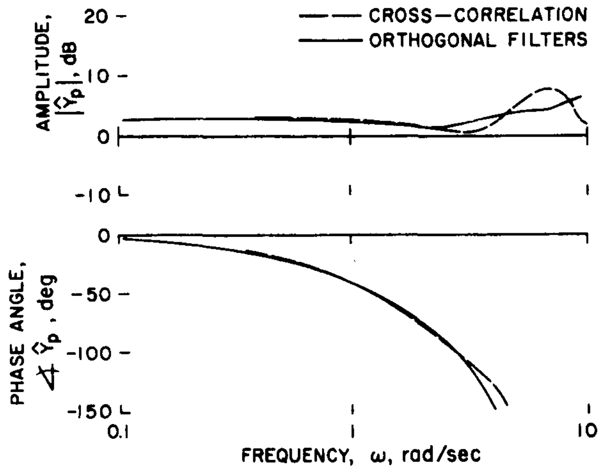

Figure 7.- Comparison of two identification methods for yaw control task during retrofire; $\lambda = 0.7$ sec.

comparison of these representative time-domain identification methods. We see that there is good agreement between the methods below the frequency of about 1 rad/sec. The major differences appear at the high frequencies. For these flight records there is very little input power at frequencies above about 2 rad/sec so the data shown at frequencies above this value probably have little significance.

The describing functions measured by both techniques, as shown in figure 7, appear to represent a constant gain system with a time constant, τ_p, of about 0.7 sec. This result, although not directly comparable to the results from previous studies, does appear reasonable. For instance, with a rate command system as used in this control task, reference 1 has shown that the pilot describing function will be essentially a constant gain system with a pure time delay. Any difference in the gain (which is lower for the flight data) and the time delay (which is higher for the flight data) appears to be attributed to the fact that in this spacecraft task the pilot is controlling about 3 separate axes whereas in reference 1 the pilot was controlling only about a single axis.

EFFECT OF TIME LAGS IN THE TOTAL CONTROL LOOP

Up to this point, we have assumed that $Y_c(j\omega)$ is minimun phase; for instance, we have not included the effect of any transport lags in $Y_c(j\omega)$. As shown in the appendix, any time delay, τ_c, in $Y_c(j\omega)$ will further tend to decrease the measurement error in $\hat{Y}_p(j\omega)$. In particular, the measurement error will theoretically be zero if

$$R_{nn}(\tau) = 0 \qquad \text{for} \qquad \tau > \lambda + \tau_c$$

where

$$\lambda \leq \tau_p$$

This means that, in general, the measurement error can be made small if the autocorrelation function of the internal noise is negligible when τ is greater than the sum of all transport lags through the total control loop, $\tau_c + \tau_p$.

This approach to system identification, as developed in this paper, indicates that the internal noise, n(t), need not be a hinderance to identification; but, rather, it may possibly aid in the identification and analysis of feedback control systems (if the conditions stated above are met). This is an important point that may also have application in many other fields (i.e., biology, economics, chemical processes) where measurements can only be made with the noise introduced internally within the system to be measured.

CONCLUDING REMARKS

This paper has shown that in measuring pilot describing functions, the measurement error due to the correlation of the input error signal with the pilot's output noise can be reduced by shifting the input data during the computer analysis. The value for this time shift should be near the effective time delay of the pilot. It is shown that this measurement error can be made small if the autocorrelation function, $R_{nn}(\tau)$, of the internal noise source is negligible for τ greater than the sum of all transport lags through the control loop. This means that if these conditions are met, it is conceivable to measure the describing function of a system with feedback using only its own internal noise source for excitation.

Representative data from the retrofire portions of the Gemini X flight demonstrate the feasibility of measuring the pilot's describing function during normal spacecraft operation. Although these data generally agree with previous simulator results, additional piloted simulator data which more accurately duplicate the actual flight control task should be obtained for comparison with future measurements of the pilot describing function during spacecraft operation.

APPENDIX

ERRORS IN IDENTIFICATION WITH OPEN-LOOP METHODS

This appendix considers the open-loop measurement error due to the correlation of $e(t)$ with $n(t)$ when the identification method is constrained to be physically realizable. Time-domain methods such as cross-correlation (refs. 2 and 3), orthogonal filters (refs. 2 and 4), and parameter trackers (refs. 2 and 5) are examples in this category.

With the constraint equation (1) of the text becomes

$$\hat{Y}_p(j\omega) = \frac{[\Phi_{ec}(j\omega)/\Phi_{ee}^-(j\omega)]_+}{\Phi_{ee}^+(j\omega)} \tag{A1}$$

where

$\Phi_{ee}(\omega) = \Phi_{ee}^+(j\omega)\,\Phi_{ee}^-(j\omega)$

$\Phi_{ee}^+(j\omega)$ has no poles or zeros in the RHP

$\Phi_{ee}^-(j\omega)$ has no poles or zeros in the LHP

$[\ ]_+$ has no poles in the RHP

This follows the usual solution (ref. 8) to the Wiener-Hopf equation which allows only a physically realizable system. That is, $\hat{Y}_p(j\omega)$ is constrained to have no poles in the RHP (right half of the real vs. imaginary plane).

Substituting the individual terms for $\Phi_{ec}(j\omega)$ we have

$$\hat{Y}_p(j\omega) = \frac{[Y_p(j\omega)\,\Phi_{ee}^+(j\omega)]_+ + [\Phi_{en}(j\omega)/\Phi_{ee}^-(j\omega)]_+}{\Phi_{ee}^+(j\omega)} \tag{A2}$$

Now we introduce the important feature of delaying $e(t)$ by an amount λ as illustrated in figure 2. The estimated transfer function can then be written:

$$\hat{Y}_p(j\omega) = \frac{e^{-\lambda j\omega}[e^{\lambda j\omega}Y_p(j\omega)\,\Phi_{ee}^+(j\omega)]_+ + e^{-\lambda j\omega}[e^{\lambda j\omega}\Phi_{en}(j\omega)/\Phi_{ee}^-(j\omega)]_+}{\Phi_{ee}^+(j\omega)} \tag{A3}$$

To simplify the following discussion let us assume that $\lambda \le \tau_p$ where τ_p is a pure time delay in $Y_p(j\omega)$. Then since $e^{\lambda j\omega}Y_p(j\omega)$ is physically realizable

$$\hat{Y}_p(j\omega) = Y_p(j\omega) + \frac{e^{-\lambda j\omega}[e^{\lambda j\omega}\Phi_{en}(j\omega)/\Phi_{ee}^{-}(j\omega)]_+}{\Phi_{ee}^{+}(j\omega)} \tag{A4}$$

The term $\Phi_{ee}(\omega)$ is made up of contributions from two sources; $i(t)$ and $n(t)$. The maximum error can be determined by assuming $i(t) = 0$ (ref. 2). With this assumption and using basic closed-loop relationships let us define

$$\Phi_{ee}^{+}(j\omega) = \frac{-Y_c(j\omega)\Phi_{nn}^{+}(j\omega)}{1 + Y_pY_c(j\omega)} \tag{A5}$$

$$\Phi_{ee}^{-}(j\omega) = \frac{-Y_c(-j\omega)\Phi_{nn}^{-}(j\omega)}{1 + Y_pY_c(-j\omega)} \tag{A6}$$

$$\Phi_{en}(j\omega) = \frac{-Y_c(-j\omega)\Phi_{nn}^{+}(j\omega)\Phi_{nn}^{-}(j\omega)}{1 + Y_pY_c(-j\omega)} \tag{A7}$$

These definitions for $\Phi_{ee}^{+}(j\omega)$ and $\Phi_{ee}^{-}(j\omega)$, which assume certain pole and zero locations in the RHP and LHP, will hold for most practical control situations except if $Y_c(j\omega)$ is a non-minimum phase (i.e., contains a time delay or zeros in RHP). A case in which Y_c is a non-minimum phase will be illustrated at the end of this appendix.

Y_c Minimum Phase

Using the foregoing assumptions, which cover a broad variety of piloted control situations, we arrive at

$$\hat{Y}_p(j\omega) = Y_p(j\omega) - \frac{e^{-\lambda j\omega}[e^{\lambda j\omega}\Phi_{nn}^{+}(j\omega)]_+}{\Phi_{nn}^{+}(j\omega)}\left[\frac{1}{Y_c(j\omega)} + Y_p(j\omega)\right] \tag{A8}$$

where $[e^{\lambda j\omega}\Phi_{nn}(j\omega)]_+$ is evaluated as $\mathfrak{F}u(t)R_{nn}(t + \lambda)$, in which u is the unit step function, and $R_{nn}(\tau)$ is the autocorrelation function of the noise, $n(t)$. The above means that the Fourier transform is only evaluated for τ greater than λ.

Equation (A8) gives the result we were after. For instance, note from this equation that if λ is positive and if $n(t)$ is white noise ($R_{nn}(\tau)$ is an impulse at $\tau = 0$), then $[e^{\lambda j\omega}\Phi_{nn}^{+}(j\omega)]_+$ is evaluated as zero and there will be no error in identification. The general requirement for the measurement error to be zero is that $R_{nn}(\tau) = 0$ for $\tau > \lambda$.

Let us further look at a more general form for $n(t)$ and let $R_{nn}(\tau) = Ke^{-\alpha|\tau|}$ and we obtain

$$\hat{Y}_p(j\omega) = Y_p(j\omega) - e^{-\alpha\lambda}\left[\frac{1}{Y_c(j\omega)} + Y_p(j\omega)\right] e^{-\lambda j\omega} \tag{A9}$$

This shows that the error term on the right side of the equation is a function of the magnitude of the constant factor $e^{-\alpha\lambda}$. As λ increases and if α is large (near white noise), then $\hat{Y}_p(j\omega) \approx Y_p(j\omega)$. Conversely, if $\lambda = 0$ then the result is identical to that shown in reference 2; $\hat{Y}_p(j\omega) = [-1/Y_c(j\omega)]$.

With Time Delay in Y_c

Any pure time delay, τ_c, in $Y_c(j\omega)$ will further reduce the measurement error. This can be shown by noting that τ_c does not affect the previous definition of $\Phi_{ee}(\omega)$ ($\Phi_{ee}(\omega)$ is not imaginary) but it will appear in the definition of $\Phi_{en}(j\omega)$. The resulting form for equation (A8) with a time delay, τ_c, in $Y_c(j\omega)$ is

$$\hat{Y}_p(j\omega) = Y_p(j\omega) - \frac{e^{-\lambda j\omega}\left[e^{(\lambda+\tau_c)j\omega}\Phi_{nn}^{+}(j\omega)\right]_+}{\Phi_{nn}^{+}(j\omega)}\left[\frac{1}{Y_c(j\omega)} + Y_p(j\omega)\right] \tag{A10}$$

It is interesting to note that in this case if $R_{nn}(\tau) = 0$ for $\tau > \tau_c$ then $Y_p(j\omega)$ does not have to have a time delay (and no time delay, λ, is required in the analysis) in order to have zero measurement error.

REFERENCES

1. McRuer, Duane; Graham, Dunstan; Krendel, Ezra; and Reisener, William Jr.: Human Pilot Dynamics in Compensatory Systems. Tech. Rep. AFFDL TR-65-15, USAF, July 1965.

2. Elkind, Jerome I.: Further Studies of Multiple Regression Analysis of Human Pilot Dynamic Response; A Comparison of Analysis Techniques and Evaluation of Time-Varying Measurements. ASD-TDR-63-618, March 1964.

3. Taylor, Lawrence W.: A Comparison of Human Response Modeling in the Time and Frequency Domains. Proc. of 3rd Annual NASA-University Conference on Manual Control. NASA SP-144, 1967, pp. 137-153.

4. Elkind, Jerome I.; Starr, Edward A.; Green, David M.; and Darley, D. Lucille: Evaluation of a Technique for Determining Time-Invariant and Time-Variant Dynamic Characteristics of Human Pilots. NASA TN D-1897, 1963.

5. Todosiev, E. P.; Rose, R. E.; Bekey, G. A.; and Williams, H. L.: Human Tracking Performance in Uncoupled and Coupled Two-Axis Systems. NASA CR-532, 1966.

6. Graham, Dunstan; and McRuer, Duane: Analysis of Non-linear Control Systems. John Wiley and Sons, N. Y., 1961.

7. McDonnell, J. D.; and Jex, H. R.: A Critical Tracking Task for Man-Machine Research Related to the Operators Effective Time Delay. NASA CR-674, 1966.

8. Newton, George C.; Gould, Leonard A.; and Kaiser, James F.: Analytical Design of Linear Feedback Controls. John Wiley and Sons, N. Y., 1957.